







# DeepSS2GO: protein function prediction from secondary structure

Fu V. Song <sup>1,\*</sup>, Jiaqi Su <sup>1</sup>, Sixing Huang <sup>2</sup>, Neng Zhang <sup>3</sup>, Kaiyue Li <sup>1</sup>, Ming Ni<sup>4,\*</sup>, Maofu Liao <sup>1,5,\*</sup>

<sup>1</sup>Department of Chemical Biology, School of Life Sciences, Southern University of Science and Technology, Xueyuan Avenue, 518055, Shenzhen, China

<sup>2</sup>Gemini Data Japan, Kitaku Oujikamiya 1-11-11, 115-0043, Tokyo, Japan

<sup>3</sup>Electronic Engineering and Computer Science, Queen Mary University of London, Mile End Road, E1 4NS, London, UK

<sup>4</sup>MGI Tech, Beishan Industrial Zone, 518083, Shenzhen, China

<sup>5</sup>Institute for Biological Electron Microscopy, Southern University of Science and Technology, Xueyuan Avenue, 518055, Shenzhen, China

\*Corresponding authors: Fu V. Song, Department of Chemical Biology, School of Life Sciences, Southern University of Science and Technology, 518055, Shenzhen, China. Tel.: +86-19820810528; E-mail: [songf@mail.sustech.edu.cn](mailto:songf@mail.sustech.edu.cn); Ming Ni, MGI Tech, 518083, Shenzhen, China. Tel: +86-13798232262;

E-mail: [niming@mgi-tech.com](mailto:niming@mgi-tech.com); Maofu Liao, Department of Chemical Biology, School of Life Sciences, Southern University of Science and Technology, Xueyuan Avenue, 518055, Shenzhen, China, and Institute for Biological Electron Microscopy, Southern University of Science and Technology, 518055, Shenzhen, China.

Tel.: +86-755-88011103; E-mail: [liaomf@sustech.edu.cn](mailto:liaomf@sustech.edu.cn)

## Abstract

Predicting protein function is crucial for understanding biological life processes, preventing diseases and developing new drug targets. In recent years, methods based on sequence, structure and biological networks for protein function annotation have been extensively researched. Although obtaining a protein in three-dimensional structure through experimental or computational methods enhances the accuracy of function prediction, the sheer volume of proteins sequenced by high-throughput technologies presents a significant challenge. To address this issue, we introduce a deep neural network model DeepSS2GO (Secondary Structure to Gene Ontology). It is a predictor incorporating secondary structure features along with primary sequence and homology information. The algorithm expertly combines the speed of sequence-based information with the accuracy of structure-based features while streamlining the redundant data in primary sequences and bypassing the time-consuming challenges of tertiary structure analysis. The results show that the prediction performance surpasses state-of-the-art algorithms. It has the ability to predict key functions by effectively utilizing secondary structure information, rather than broadly predicting general Gene Ontology terms. Additionally, DeepSS2GO predicts five times faster than advanced algorithms, making it highly applicable to massive sequencing data. The source code and trained models are available at <https://github.com/orca233/DeepSS2GO>.

**Keywords:** protein function prediction; secondary structure; deep learning; sequence-based method; homology identification

## INTRODUCTION

Proteins are vital for a wide range of biological processes, serving key roles in cellular functions across both prokaryotic and eukaryotic organisms. An in-depth understanding of protein function not only has a considerable impact on meeting the academic demand for life science, but also drives advancements in the field of biomedicine [1]. Protein function annotation can be achieved through biochemical experiments or computational methods. While the former is the gold standard due to its high

accuracy and reliability, it is costly and low-throughput, making it unsuitable for the vast amount of protein sequence data generated by high-throughput sequencing instruments [2]. Therefore, there is a pressing need to develop theoretical computational methods that combine accuracy with efficiency in protein function prediction [3].

Currently, there are multiple protein function classification standards, including Gene Ontology (GO) [4], EC [5], KEGG [6], Pfam [7, 8], etc. Among these, the GO database is widely recognized

**Fu Song** is a Research Assistant Professor at Southern University of Science and Technology. His research interests include bioinformatics, deep learning, protein function and structure prediction.

**Jiaqi Su** is a PhD student in the School of Life Science at Southern University of Science and Technology. His research interests lie in computer aided drug design, protein design, deep learning and graph neural network.

**Sixing Huang** is a data scientist at Gemini Data Japan. His research interests include knowledge graphs and bioinformatics.

**Neng Zhang** is a PhD student in the School of Electronic Engineering and Computer Science at Queen Mary University of London. His research interests include deep learning, computer vision, camera calibration and semantic segmentation.

**Kaiyue Li** is a PhD student in the School of Life Sciences at Southern University of Science and Technology. Her research interests include EM structure and molecular mechanism.

**Ming Ni** is a senior engineer and vice president at MGI. His research interests include systems biology, high-throughput sequencing technology and single-cell omics.

**Maofu Liao** is a full-time professor at the Southern University of Science and Technology. His research interests include cryo-EM structures and molecular mechanisms of membrane protein complexes.

Received: January 24, 2024. Revised: March 31, 2024. Accepted: April 10, 2024

© The Author(s) 2024. Published by Oxford University Press.

This is an Open Access article distributed under the terms of the Creative Commons Attribution Non-Commercial License (<https://creativecommons.org/licenses/by-nc/4.0/>), which permits non-commercial re-use, distribution, and reproduction in any medium, provided the original work is properly cited.

For commercial re-use, please contact [journals.permissions@oup.com](mailto:journals.permissions@oup.com)

for its relative comprehensiveness and systematic approach to describing the biological aspects of Molecular Function Ontology (MFO), Cellular Component Ontology (CCO) and Biological Process Ontology (BPO). The GO database is structured as a directed acyclic graph (DAG) with 'is-a' or 'part-of' relationships between GO terms, efficiently capturing protein functional characteristics [4]. Meanwhile, if a protein is annotated with a GO term, all its ancestor terms up to the root of the ontology should also be annotated.

Protein function prediction methods can be categorized by the information utilized or the algorithms employed [9, 10]. Information-based categorization includes methods grounded on primary sequence, tertiary structure or protein-protein interaction (PPI) [11]. Algorithm-based categorization includes methods relying on sequence homology alignment (e.g. BLAST [12, 13], InterProScan [14], Multiple Sequence Alignment [15] and Position-Specific Scoring Matrix (PSSM) [16]) and those based on deep learning (e.g. Convolutional Neural Networks (CNNs) [17], Graph Neural Network (GNN) [18], Diffusion Network [19], Transformer [20, 21], Large Language Models [22], etc). These two classification schemes intersect with each other. For instance, methods that rely on extracting primary sequence features can utilize various techniques, such as DeepPPIISP [23] with PSSM, DeepGOPlus [24] employing CNN and TALE [25] with transformer architecture. Additionally, methods like Graph2GO [26] and DeepFRI [27], leverage GNN to utilize the three-dimensional (3D) structure. Furthermore, NetGO [28] harnesses PPI network information from the STRING database [29] for protein function prediction. Lastly, researchers often integrate multiple sources of information, such as combining protein sequence features with protein network information, as seen in the DeepGraphGO [30] approach.

Determining the relevant biological data and extracting essential features for model training is crucial beyond the variety of algorithms. This process is fundamental in leveraging biological information effectively. The essence of protein function prediction lies in learning the relationship between various biological information features and known functional labels within established species. This process is not about creating new GO terms; the predicted functions are inherently part of the existing functional pool. When confronted with unknown proteins, the trained model is employed in conjunction with the biological features of these proteins to score all the GO terms in the functional pool. The biological features of primary sequences encapsulate the patterns of the 20 amino acids. Different lengths and sequence orders correspond to diverse functions. Conversely, the biological features associated with tertiary structures pertain to spatial shapes, where distinct shapes and size features reveal critical insights and identify different functions.

According to the thermodynamic hypothesis proposed by Christian Anfinsen [31], the amino acid sequence dictates the protein tertiary structure, which is directly linked to its function. Therefore, incorporating 3D structural features is expected to improve the accuracy of protein function annotation, and many algorithms have also demonstrated this [26, 27]. However, limitations of introducing 3D structures persist. While wet laboratory methods for analyzing protein 3D structures deliver accurate and reliable outcomes [32, 33], they are not sufficient to accommodate the demands of predicting functions from a large influx of new sequences [34], also entailing substantial financial and temporal costs [35]. While computational methods like AlphaFold2 [36] and trRosetta [37] have reduced this

prediction time to a matter of hours, 3D-based function prediction methods still fall short of efficiently handling the vast amount of sequencing data produced by high-throughput sequencing instruments. Consequently, although methods that combine multiple sources of information typically outperform those solely relying on sequence data, obtaining these additional pieces of information in a short time frame is challenging. It may not be applicable to predict the function of less-studied proteins.

In cases where an abundance of primary sequences is available but tertiary structures are lacking, secondary structures exhibit distinct advantages. While primary sequences may vary significantly among different species, secondary structures, by eliminating redundant information, allow for a more focused investigation into the arrangement patterns of modules.

Secondary structures can be classified into eight categories according to the Dictionary of Secondary Structure of Proteins (DSSP) [38, 39]: alpha-helix (H), 310-helix (G), pi-helix (I), beta-strand (E), beta-bridge (B), hydrogen-bonded turn (T), bend (S) and Coil (C). Although some research integrates protein secondary structure information as input features, like GAT-GO [40] and SSEalign [41], the application of secondary structure information has historically been constrained by data quality and quantity. We employ modified SPOT-1D-LM suite [42] to predict secondary structures for 68 325 primary sequences from SwissProt including all species in 20 h, offering accuracy and speed suitable for processing large-scale datasets. Details will be illustrated in the Materials and Methods section in Table 1.

Notably, relying solely on secondary structure predictions remains insufficient for protein function prediction because of two reasons: First, this is due to variations in the amino acid arrangement of similar  $\alpha$  helices (H, G, I) and  $\beta$  sheets (E, B), resulting in differences in physicochemical properties like charge and hydrophobicity. Secondly, intrinsically disordered protein regions, which play a critical role in alternative splicing, folding and catalytic reactions [43], will be indiscriminately labeled with the secondary structure tag of Coil (C), thus failing to precisely differentiate between various functions. Consequently, we require the primary sequence and the homology information obtained through the Diamond algorithm [44] as a more refined supplement to the coarse secondary structure feature.

In this study, we propose a protein function predictor DeepSS2GO (Secondary Structure to Gene Ontology). This method utilizes deep learning models to extract features from the secondary structure and supplements them with primary sequence and homology information. This algorithm combines the sequence-based speed with the structure-based accuracy while also overcoming shortcomings like streamlining the redundant information in primary sequences and avoiding the time-consuming issue associated with tertiary structure analysis. When compared with similar algorithms, DeepSS2GO demonstrates superior performance in the MFO and CCO while achieving the second place in the BPO on both the Maximum F-measure ( $F_{max}$ ) and Area Under the Precision-Recall Curve (AUPR) evaluation criterion. Furthermore, it attains the highest ranking in all three sub-ontologies when evaluated using the Minimum Sensitivity Index ( $S_{min}$ ) criterion. Notably, it accelerates computational speed by 5-fold [45]. Through two case analyses, we validate the efficacy of our approach in accurately predicting key functions of non-homologous proteins, providing comprehensive coverage. Moreover, the reduced training duration of our model facilitates prompt revisions of the SwissProt and GO databases, enhancing the timeliness of database updates.

**Table 1:** The number of protein sequences in the training-testing sets and the number of GO term classes grouped by sub-ontologies. Datasets include SwissProt, CAFA3 and training HUMAN testing other species. Detailed information on training one species and testing other species can be found in [Supplementary Table S1](#)

	Training					Testing					Terms classes			
	MFO	CCO	BPO	Total		MFO	CCO	BPO	Total		MFO	CCO	BPO	Total
SwissProt	38 530	51 022	51 079	68 325	SwissProt	1954	2643	2657	3597	700	576	3965	5241	
CAFA3	32 090	45 080	45 715	60 372	CAFA3	1046	1294	2095	3049	514	355	2643	3512	
HUMAN	9125	12 037	10 151	13 238	ARATH	5038	7352	7225	10 002	336	217	1293	1846	
HUMAN	9125	12 037	10 151	13 238	ECOLI	2267	2228	2525	3288	265	74	792	1131	
HUMAN	8677	11 447	9644	12 576	HUMAN	448	590	507	662	302	269	1517	2088	
HUMAN	9125	12 037	10 151	13 238	MOUSE	5382	7977	8201	10 152	389	347	2509	3245	
HUMAN	9125	12 037	10 151	13 238	MYCTU	563	1133	732	1456	189	46	617	852	
HUMAN	9125	12 037	10 151	13 238	YEAST	3191	4730	4256	4964	335	247	1267	1849	

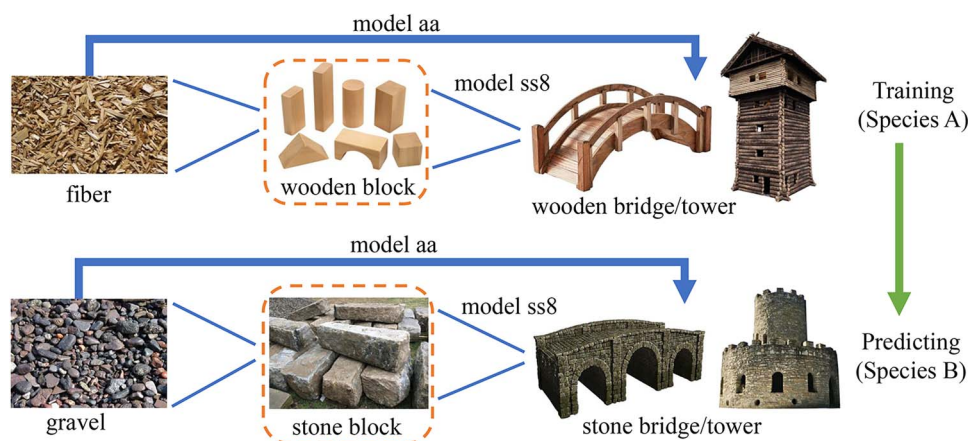


**Figure 1.** Overview of the DeepSS2GO conceptual diagram. This concept parallels two sets: 'fiber - wooden block - wooden bridge' and 'gravel - stone block - stone bridge', comparing them with the protein primary sequence - secondary structure - tertiary/quaternary structures. Traditional methods predict functions (bridge or tower), by studying the arrangement patterns of fiber or gravel (primary sequence features). This study introduces a new approach by examining the arrangement patterns of wooden blocks (secondary structure features) to predict functionality.

## MATERIALS AND METHODS

### Overview

The overall concept and idea of the DeepSS2GO algorithm is illustrated in [Figure 1](#). The primary sequence is analogous to fiber/gravel, the secondary structure to wooden/stone block and the tertiary-quaternary structure to a wooden/stone bridge or tower. Traditional sequence-based prediction methods (model-aa) study the arrangement patterns of fiber and their relationship to the macroscopic object functional label as bridge or tower. However, due to potential differences in the arrangement of fibers and gravel, it might be difficult to predict whether it is a bridge or a tower. In situations where 3D spatial coordinates are not readily available, this study, instead of focusing on the arrangement of fibers, investigates the arrangement of intermediate wooden blocks and their relationship (model-ss8) to the macroscopic object functional label. Theoretically, compared with primary sequences, the model trained on secondary structures possesses greater translational capability, especially for cross-species predictions.

### Datasets

In this study, the functional annotations were derived from the GO [4] (June 2023), encompassing a comprehensive dataset distributed across three domains, including 47 497 terms: MFO (12 480), CCO (4474) and BPO (30 543). Referencing the experiences

from other studies [24, 45, 46], to enhance training efficiency and prediction accuracy, our training approach focused exclusively on GO terms with a sufficient number of training samples (i.e. the same GO label appearing in  $\geq 50$  sequences). Furthermore, annotations were propagated utilizing the relationships within the GO hierarchy [46].

Two datasets were employed in this research: SwissProt [47] (April 2023) and Critical Assessment of Function Annotation Challenge (CAFA3) [24]. SwissProt, a subset of the UniProt database, is meticulously curated and manually annotated. Protein sequences and GO annotations used in this study are collected from SwissProt, retaining only experimental GO annotations with evidence codes IDA, IPI, EXP, IGI, IMP, IEP, IC or TA. A total of six major species are selected for cross-validation training-testing: *Arabidopsis thaliana* (ARATH, 10 002), *Escherichia coli* (ECOLI, 3288), *Homo sapiens* (HUMAN, 13 238), *Mus musculus* (MOUSE, 10 152), *Mycobacterium tuberculosis* (MYCTU, 1456) and *Saccharomyces cerevisiae* (YEAST, 4964).

The selection of these six species was primarily based on two reasons: First, the choice was to include species with a relatively large number of sequences, ensuring an ample amount of data for training and testing. The six selected species are all ranked within the top 10 in terms of total quantity. Secondly, it was important to select species that include both closely related and significantly divergent organisms. This approach helps to reduce

bias in horizontal comparisons, demonstrating the superiority of the ss8 model over the aa model across various cross-validation evaluations. Among the selected species, some exhibit close similarities, such as HUMAN VS. MOUSE and ECOLI VS. MYCTU. Conversely, some show substantial differences, such as HUMAN VS. ARATH, and eukaryotes VS. prokaryotes.

Table 1 illustrates detailed statistics of the training and testing sets for the three domains in GO, including the number of proteins and GO labels. The datasets include SwissProt, CAFA3 and training HUMAN testing other species. Detailed information on training one species and testing other species can be found in [Supplementary Table S1](#). Additionally, to facilitate comparisons with other cutting-edge protein function prediction methodologies [46], CAFA3 [24] dataset is used for both training-testing sequences and functional annotations. Modified SPOT-1D-LM algorithm [42] is employed to predict secondary structures from primary amino acid sequences. Given that this algorithm utilizes the ESM-1b [21] and Prottrans [48] pre-trained models, it is constrained by protein length (less than 1024). After screening, a total of 68 325 protein sequences for Swissprot and 60 372 for CAFA3 were retained.

## The architecture of DeepSS2GO

The overall architecture is shown in [Figure 2A](#). DeepSS2GO comprises three modules: two deep learning modules, one focused on secondary structures and the other on primary sequences, and a third module oriented toward homology alignment.

### Overall framework

The process begins by obtaining primary sequences and manually propagated annotations that have been filtered from the SwissProt training set, shown as the initial input in [Figure 2A](#). Subsequently, data preprocessing is conducted. The altered SPOT-1D-LM suite is employed to convert primary amino acid sequences into secondary structures in bulk, i.e. replacing the original 20 amino acid letters with eight letters representing secondary structures (H, G, I, E, B, T, S, C) [38, 39]. Then, both the primary sequences and secondary structures are fed into the deep learning model ([Figure 2B](#)), respectively, yielding initial predictions for pred-aa and pred-ss8. On the other hand, homology comparison result Pred-bit-score is performed using the Diamond method [44], a remarkably high-speed and high-performance tool for conducting protein homology searches. The final prediction score is calculated by combining the three prediction scores ( $S_{aa}$ ,  $S_{ss8}$ , and  $S_{Diamond}$ ) through Equation 1, where  $\alpha$  and  $\beta$  are two hyperparameters balancing the influence of the three components, satisfying the following conditions:  $0 \leq \alpha \leq 1$ ,  $0 \leq \beta \leq 1$  and  $0 \leq \alpha + \beta \leq 1$ .

$$S(p, f) = \alpha * S_{aa} + \beta * S_{ss8} + (1 - \alpha - \beta) * S_{Diamond} \quad (1)$$

### Setup of model

As both primary sequences and secondary structures are one-dimensional linear data structures, we employed the same deep-learning model for both. To highlight the advantages and effectiveness of secondary structures and to restore the biological essence as much as possible, we employ the most classic and concise CNN to extract their features.

We utilize PyTorch [49] to construct our neural network models, as depicted in [Figure 2B](#). For a given protein sequence, we first convert the input primary sequence or secondary structure sequence into a one-hot matrix. If the input is a primary amino acid sequence, the matrix size will be [1024, 21], where the width

21 represents the 20 types of amino acids plus 'other'. If the input is a secondary structure, the matrix size will be [1024, 9], where width 9 represents the eight types of secondary structures plus 'other'. 1024 is the length of the input, and sequences shorter than 1024 are padded with zeros. The input is then passed through a series of CNN layers with varying kernel sizes and filters, followed by Max Pooling layers, and normalized to the scoring range [0, 1] for n types of GO terms individually through the Sigmoid function. The training of a single model concludes within a maximum of 50 epochs. Additionally, we employed an EarlyStopping strategy with the patience of six epochs to prevent overfitting.

Given the considerable parameter search space, after establishing certain hyperparameters such as the loss function (Binary Cross Entropy Loss), optimizer (Adam [50]), learning rate (0.0003) and activation function (Sigmoid), we focused on studying the parameters of kernel and filter size, which are more sensitive to protein function. These parameters will determine the features of specific sequences of particular sizes. Our model explores different combinations of kernels and filters, with kernel size varying between 8 and 128 in increments of 8, whereas the filter size ranges from 16 to 65 536, doubling with each step.

The model-aa and model-ss8 are trained separately, and evaluated on the respective testing dataset for MFO, CCO and BPO, thus determining the optimal kernel and filter size for each sub-ontology. The predicted GO scores by the best model, Pred-aa or Pred-ss8, will be combined with Pred-bit-score to yield the Final-score. Regarding the design of the model framework, we have also attempted to add fully connected layers after Max Pooling and represent secondary structures with three letters, but neither approach was satisfactory. Therefore, we will not elaborate further here.

## Implementation

We conduct two categories of experiments: specified cross-species testing, and testing that includes all species. To validate the enhanced translational ability of models trained on secondary structures, we employ cross-species testing, i.e. training with species A and testing with species B. To maximize primary sequence diversity, we aim to select species with significant distinctions, even using prokaryotic and eukaryotic organisms as separate training and testing sets. From SwissProt, six different species (ARATH, ECOLI, HUMAN, MOUSE, MYCTU, YEAST) are chosen for mutual testing. This selection includes two prokaryotes and four eukaryotes, the latter encompassing animals, plants and fungi.

For the comprehensive species testing, the CAFA3 dataset is utilized for benchmarking against other similar algorithms, and the entire SwissProt dataset is employed to develop a model as complete and extensive as possible for predicting protein functions in new species. Specific details of the data can be found in the [Datasets](#) section.

If training and testing are conducted on the same species A (or the whole-species SwissProt dataset), then a random 5% of species A data is used as the testing set, with the remaining 95% as the training set. In contrast, if different species are used for training and testing, i.e. training on species A and testing on species B, then 100% of species A data is used as the training set, and 100% of species B data as the testing set. In both cases, 10% of the training set is allocated for validation during training. For instance, as shown in [Table 1](#), there are a total of 13 238 HUMAN proteins and 10 002 ARATH proteins. If both training and testing are performed using HUMAN, then 12 576 proteins (95%) are used for the training set and 662 proteins (5%) for the testing set. If training HUMAN

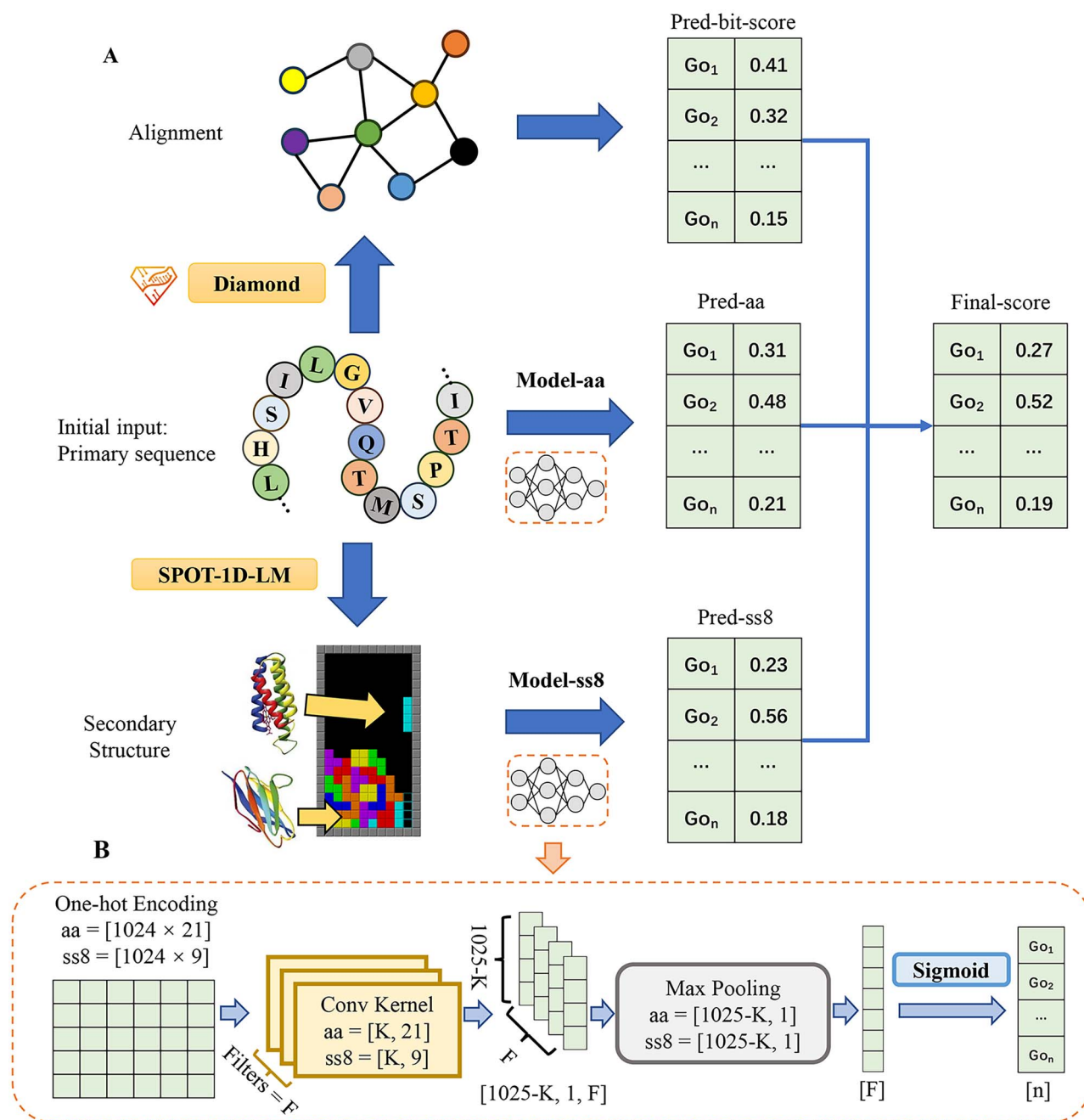


**Figure 2.** (A) The architecture of DeepSS2GO. The model consists of three components: a model trained on secondary structures (model-ss8), a model trained on primary sequences (model-aa) and Diamond homology alignment. First, the input primary sequence is converted into a secondary structure. Then, the primary sequence and secondary structure are separately processed through deep learning models to obtain preliminary predictions, Pred-aa and Pred-ss8. These, combined with the Pred-bit-score predicted by Diamond, are integrated to yield the Final-score. (B) The setup of model-aa and model-ss8. The input is a one-hot matrix, which passes through convolutional layers and pooling layers. After that, each term in the GO pool is scored individually using the Sigmoid activation function. For the one-hot matrices based on primary sequences and secondary structures, the sizes of the convolutional kernels and max pooling slightly differ. Kernel size ranges from 8 to 128 in increments of 8, while filter size ranges from 16 to 65 536, doubling with each increment.

and testing ARATH, then all 13 238 HUMAN proteins are used as the training set, and all 10 002 ARATH proteins as the testing set. In total, we conducted 76 (i.e.  $36 \times 2 + 4$ ) sets of tests, including cross-training/testing among the six species, and all-species dataset of SwissProt/CAFA3, for both aa and ss8. All training and testing processes are carried out on a Linux system equipped with a 24GB Nvidia GeForce RTX 3090.

## Evaluation metrics

Referring to relevant studies in this field [45, 46], we adapt three metrics for performance evaluation:  $F_{\max}$ , AUPR and  $S_{\min}$  [51–53].  $F_{\max}$  is a metric that integrates precision and recall. The F-measure is the harmonic mean of precision and recall.  $F_{\max}$  is the maximum F-measure achieved across all potential threshold settings, reflecting the optimal balance between precision and

recall.

$$pr_i(t) = \frac{\sum_f I(f \in P_i(t) \wedge f \in T_i)}{\sum_f I(f \in P_i(t))} \quad (2)$$

$$rc_i(t) = \frac{\sum_f I(f \in P_i(t) \wedge f \in T_i)}{\sum_f I(f \in T_i)} \quad (3)$$

$$AvgPr(t) = \frac{1}{m(t)} \cdot \sum_{i=1}^{m(t)} pr_i(t) \quad (4)$$

$$AvgRc(t) = \frac{1}{n} \cdot \sum_{i=1}^n rc_i(t) \quad (5)$$

$$F_{max} = \max_t \left\{ \frac{2 \cdot AvgPr(t) \cdot AvgRc(t)}{AvgPr(t) + AvgRc(t)} \right\} \quad (6)$$

In this context,  $f$  represents a GO class,  $T_i$  denotes the set of true annotations,  $P_i(t)$  refers to the predicted annotations set for a protein  $i$  at a specific threshold  $t$ ,  $m(t)$  indicates the count of proteins that have at least one predicted category,  $n$  is the overall count of proteins and  $I$  is a function that returns 1 if its given condition holds true, otherwise it returns 0.  $AvgPr(t)$  and  $AvgRc(t)$  represent the average precision and average recall at thresholds  $t$ , and calculated from  $pr_i$  and  $rc_i$  by the above formulas.

AUPR is the area under the precision-recall curve across all potential thresholds. It is a powerful tool for evaluating model performance in imbalanced datasets, especially when there is a substantial disparity in the number of positive and negative samples. Compared with the traditional Receiver Operating Characteristic Curve (ROC), AUPR is more sensitive to the predictive performance of a model for the minority class. This metric reflects a model's ability to correctly identify positive (minority) instances amidst a large number of negatives (majority instances), focusing on precision and recall. In such contexts, AUPR is sensitive because it penalizes models more heavily for misclassifying the rare positive cases, thus providing a truer assessment of model performance on imbalanced datasets. It prioritizes the accurate detection of the minority class, highlighting the model's effectiveness where it is most needed.

$S_{min}$ , focusing on the minimum sensitivity index, a calculation of the gap between the true positive rate and the false positive rate across thresholds, sharply evaluates a classifier's discriminative power between positive and negative instances. This metric is particularly insightful for assessing how well a model can differentiate between classes under varying conditions. A lower  $S_{min}$  indicates a model's struggle to separate positive from negative cases effectively, often resulting in higher misclassification rates of crucial instances. In contrast, a higher  $S_{min}$  suggests that the model has a stronger capability to discern between the two, thereby reducing the likelihood of false positives and negatives. This sensitivity makes  $S_{min}$  an invaluable tool for model evaluation, especially in scenarios where the cost of misclassification is high. It pushes for models that not only recognize patterns but do so with a precision that minimizes the overlap between class distributions, enhancing the reliability of predictions in practical applications.

$$IC(c) = -\log(Pr(c|P(c))) \quad (7)$$

$$ru(t) = \frac{1}{n} \sum_{i=1}^n \sum_{c \in T_i - P_i(t)} IC(c) \quad (8)$$

$$mi(t) = \frac{1}{n} \sum_{i=1}^n \sum_{c \in P_i - T_i(t)} IC(c) \quad (9)$$

$$S_{min} = \min_t \sqrt{ru(t)^2 + mi(t)^2} \quad (10)$$

The information content,  $IC(c)$ , is determined by the likelihood of annotations for class  $c$ . Here,  $P(c)$  represents the collection of parent classes for class  $c$ .  $S_{min}$  is derived using the equations below, where  $ru(t)$  represents the average residual uncertainty, and  $mi(t)$  denotes the average misinformation.

## RESULTS

This section encompasses the following aspects: First, we validate the superiority of secondary structures over primary sequences in predicting functions by conducting cross-training predictions on proteins from different species. Secondly, we compare DeepSS2GO with other state-of-the-art methods, demonstrating the accuracy, efficiency and updating convenience of our algorithm. Thirdly, we perform ablation experiments on the techniques used in DeepSS2GO. Finally, we conduct two case studies to verify the effectiveness, efficiency and comprehensiveness of the algorithm in predicting key functions.

### Superiority of secondary structures

Using the training and testing of all SwissProt data as an example, each training set employs either primary amino acid sequences or secondary structures as inputs. After training and evaluation, we can obtain results derived from primary amino acid sequences (see [Supplementary Figure S1](#)) and results stemming from secondary structures (see [Supplementary Figure S2](#)). Each figure comprises nine subfigures representing the evaluation results of three parameters:  $F_{max}$ , AUPR and  $S_{min}$ , across three sub-ontologies: MFO, CCO and BPO. The horizontal axis represents the logarithmic value of the filter size, and the vertical axis corresponds to the parameter values, with each plot representing the same kernel size. The extremum values of these three metrics will be discussed in the Ablation study section.

For any fixed kernel, both  $F_{max}$  and AUPR values first increase and then decrease as the filter size rises. Reduction usually indicates overfitting. In the analysis with primary amino acid sequences, the peak  $F_{max}$  values observed for MFO, CCO and BPO stand at 0.528, 0.666 and 0.426, respectively. These are achieved with kernel 16 and filter 32 768. When considering secondary structures, the maximum  $F_{max}$  values for MFO and BPO reach 0.616 and 0.452, respectively, both realized with kernel 32 and filter 32 768. In contrast, CCO highest  $F_{max}$  of 0.664 is attained with kernel 48 and filter 16 384. Comparatively, the model relying on secondary structures shows superior  $F_{max}$  values, exceeding the primary sequence model by 16.7% and 6.1% in MFO and BPO sub-ontologies, while matching performance in CCO.

Similarly, in AUPR, the secondary structure algorithm outperforms the primary sequence by 19.6% and 9.3% in MFO and BPO, respectively, and is on par in CCO. In  $S_{min}$ , the secondary structure algorithm is higher by 13.4%, 1.1% and 3.2% in MFO, CCO and BPO, respectively. It is evident that the model based on secondary structures is markedly more effective in predicting the actual functions of proteins (MFO and BPO) compared with the primary amino acid sequence model. The two models perform comparably in determining protein components (CCO).

In addition to testing the whole SwissProt dataset, we select six species from SwissProt for cross-training and testing, as introduced in the [Implementation](#) section. Extracting the highest  $F_{max}$  values from the cross-validation of six different species, we obtained [Figure 3](#) (AUPR and  $S_{min}$  results can be found in

**Table 2:** Performance comparison of DeepSS2GO against five state-of-the-art methods using the CAFA3 benchmark datasets

Methods	Fmax			AUPR			Smin		
	MFO	CCO	BPO	MFO	CCO	BPO	MFO	CCO	BPO
DiamondScore	0.509	0.557	0.427	0.340	0.335	0.267	9.031	8.198	22.860
DeepGOCNN*	0.420	0.607	0.378	0.355	0.616	0.323	9.711	8.153	24.234
TALE+	0.558	0.622	0.480	0.539	0.595	0.427	8.360	7.822	22.549
DeepGOPlus*	0.544	0.623	0.469	0.487	0.627	0.404	8.724	7.823	22.573
MMSMAPlus	0.595	0.622	<b>0.535</b>	0.559	0.601	<b>0.470</b>	7.922	7.631	22.202
DeepSS2GO	<b>0.601</b>	<b>0.643</b>	0.518	<b>0.559</b>	<b>0.634</b>	0.441	<b>6.709</b>	<b>7.037</b>	<b>18.753</b>

Note: Models with \* are referenced from associated literature [24]. The best results are in bold.

**Table 3:** Assessment of the impact of different components within DeepSS2GO

aa	ss8	Diamond	Fmax			AUPR			Smin		
			MFO	CCO	BPO	MFO	CCO	BPO	MFO	CCO	BPO
✓			0.528	0.666	0.426	0.511	0.696	0.376	9.365	10.119	39.989
	✓		0.616	0.664	0.452	0.597	0.691	0.407	8.174	10.066	38.951
		✓	0.643	0.657	0.514	0.525	0.514	0.381	8.085	9.620	37.079
✓		✓	0.655	0.698	0.527	0.660	0.732	0.484	7.951	9.206	36.413
	✓	✓	0.666	0.695	0.531	0.669	0.727	0.487	7.709	9.206	36.183
✓	✓	✓	<b>0.670</b>	<b>0.703</b>	<b>0.535</b>	<b>0.674</b>	<b>0.742</b>	<b>0.493</b>	<b>7.682</b>	<b>9.072</b>	<b>36.138</b>

Note: 'aa' symbolizes the model based on the primary amino acid sequence, and 'ss8' denotes the model based on the secondary structure. The best results are in bold.

Supplementary Figures S3 and S4). In Figure 3, subfigures A, C, E represent predictions based on primary amino acid sequences (aa), while B, D, F represent predictions based on secondary structures (ss8). The same color in the upper and lower figures corresponds to the same GO sub-ontology, with subfigures A and B representing MFO, C and D representing CCO and E and F representing BPO. In each figure, a darker color indicates a higher  $F_{max}$  value.

The following observations are noted: In examining the same subplot, aligning along the diagonal, the  $F_{max}$  values for self-testing consistently rank highest. Furthermore, the approach of training on eukaryotes and testing on prokaryotes demonstrates superior performance compared with the inverse. This disparity may be due to the more substantial sample size in eukaryotic training sets, potentially enhancing model accuracy.

Upon comparing the outcomes between aa and ss8, the subfigures G, H and I of Figure 3 focus on the percentage increase in performance when transitioning from aa-trained models to ss-trained models within MFO, CCO and BPO, respectively. The red colors in the heatmaps signify a percentage increase in performance, while the blue colors indicate a decrease. For MFO, ss8- $F_{max}$  shows a notable improvement, approximately 5–20% higher than aa. This highlights the considerable advantage of secondary structures over primary sequences in the GO prediction of Molecular Function. Regarding CCO, ss8- $F_{max}$  values are marginally lower, around 1–2% than those of aa. This indicates that aa encompasses more comprehensive CCO information density compared with ss8. In the context of BPO, ss8- $F_{max}$  values generally outperform those of aa, with an increase of about 4–10%. An exception is observed in the scenario involving training on prokaryotes (ECOLI, YEAST) and testing on ARATH, where aa and ss8 yield comparable results.

The conclusions drawn from the AUPR and  $S_{min}$  (Supplementary Figures S3 and S4) analyses align with these observations. It is evident that secondary structures offer a clearer advantage in the prediction of protein functions. This is underlined by the fact that the structure dictates functions; secondary structures provide

more structural information than primary sequences, enhancing their predictive capability for functions.

## Comparison with the state-of-the-art methods

Relying solely on primary sequences falls short in protein function prediction. To solve this issue, we integrate equation 1 with secondary structure predictions, primary sequence data and alignment score assessments for a holistic approach to function annotation. This section uses the CAFA3 dataset [24] for both training and testing components, facilitating comparative analysis of the DeepSS2GO algorithm against five other sequence-based methods: DiamondScore [24], DeepGOCNN [24], TALE+ [25], DeepGOPlus [24] and MMSMAPlus [46]. The effectiveness of different algorithms is showcased through their best  $F_{max}$ , AUPR and  $S_{min}$  values across three sub-ontologies MFO, CCO and BPO, as illustrated in Table 2.

Our model, despite leveraging the most traditional CNNs, still achieves excellent results, enhancing the protein function prediction performance on the CAFA3 dataset. Table 2 highlights DeepSS2GO superior performance in MFO and CCO for the metrics  $F_{max}$  and AUPR, and its near-best results in BPO. In terms of the  $S_{min}$  metric, it excels in all three sub-ontologies. The subsequent section (Case 2), delves into the functional prediction of the protein LYP2\_MOUSE, emphasizing how the algorithm predicts specific sub-classes of GO functions and compares with other methodologies, underscoring the advantage of extracting features from protein secondary structures for predicting their functions.

Moreover, DeepSS2GO stands out for its high predictive accuracy coupled with computational efficiency. On average, the algorithm processes 1000 proteins from CAFA3 testing dataset in just 1.2 min, a substantive improvement over the cutting-edge algorithm, which requires approximately 7 min for 1000 proteins [45]. This quintuple increase in speed is particularly beneficial when analyzing large volumes of sequenced, unknown metagenomic proteins.

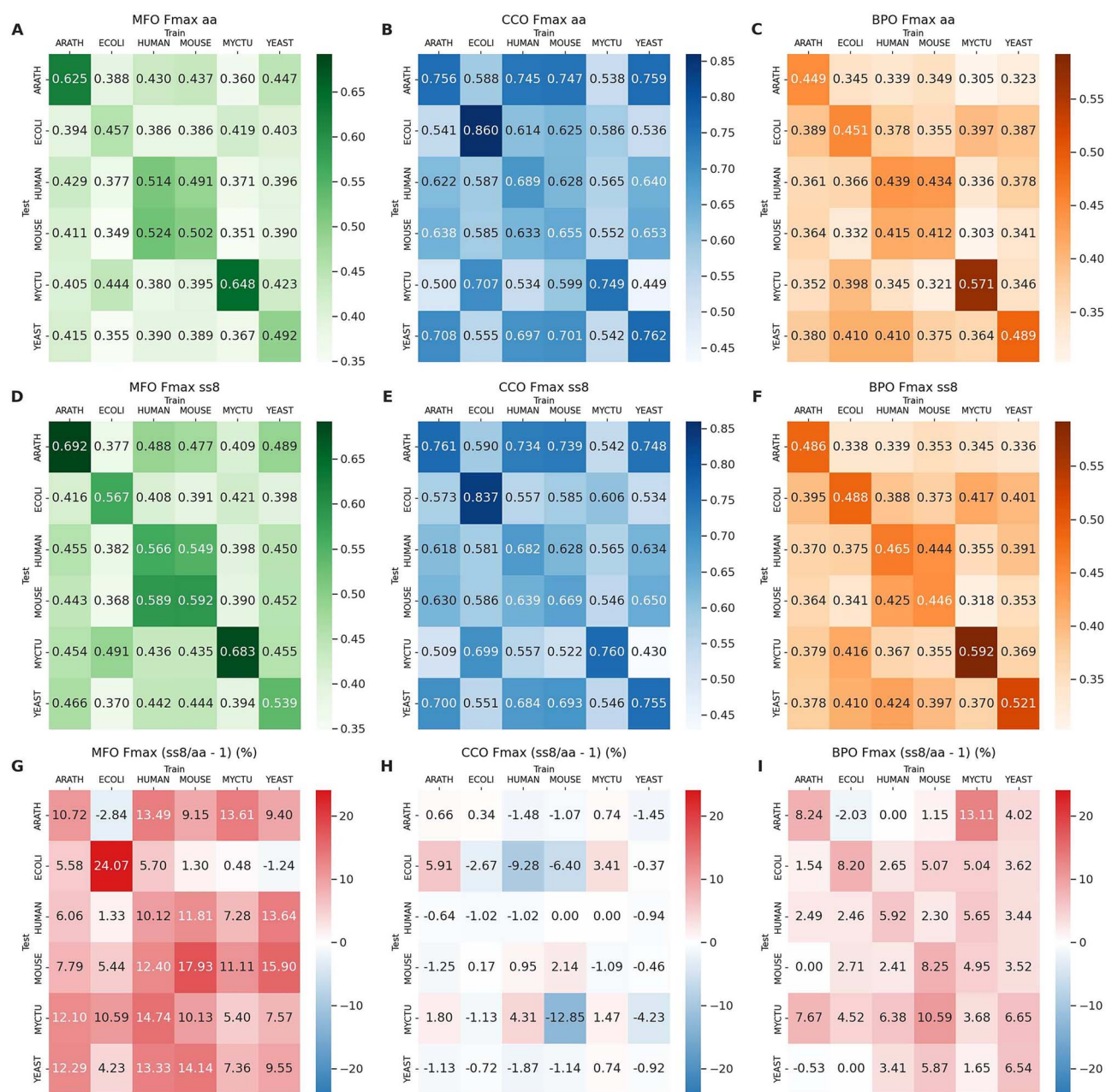


**Figure 3.** The performance of  $F_{max}$  scores in predicting GO functional annotations across species is depicted through heatmaps, utilizing models that have been trained and tested among six different species: *Arabidopsis thaliana* (ARATH), *Escherichia coli* (ECOLI), *Homo sapiens* (HUMAN), *Mus musculus* (MOUSE), *Mycobacterium tuberculosis* (MYCTU) and *Saccharomyces cerevisiae* (YEAST). (A) and (D) present MFO results based on model-aa and model-ss8, respectively; (B) and (E) show CCO results and (C) and (F) illustrate BPO outcomes. The darker shades in the color gradients indicate higher metrics scores, reflecting greater prediction accuracy. Each matrix cell provides a metrics score for a model trained on the species denoted at the top and tested on the species labeled on the side. (G) depicts the percentage increased performance from model-aa to model-ss8 in MFO, similarly, (H) and (I) represent the increments in CCO and BPO, respectively. Red indicates the percentage of increase, while blue represents the percentage of decrease.

In addition, the simplicity and user-friendliness of the model also mean that retraining costs are minimized. With continuous updates to the SwissProt and GO databases, our approach allows for rapid retraining to integrate new GO terms and discard outdated ones.

To sum up, the DeepSS2GO algorithm not only surpasses comparable methods in enhancing prediction performance on the CAFA3 dataset but also brings a substantial increase in processing speed. Furthermore, it provides a straightforward and update-friendly solution for adapting to the evolving landscape of protein and GO databases.

## Ablation study

We conduct ablation studies to demonstrate the efficacy of the three modules: aa, ss8 and Diamond, in the proposed DeepSS2GO framework (Figure 2A). Here, 'aa' symbolizes the model based on the primary amino acid sequence, and 'ss8' denotes the model based on the secondary structure. For a universally applicable validation model, we utilize the entire SwissProt database for both training and testing. Six sets of experiments were carried out, each involving different combinations of the three modules.

The findings deduced from the data presented in Table 3 can be summarized as follows: Initially, it is evident that the



simultaneous presence of all three modules yields the best results, as highlighted in bold. The optimal values for  $F_{\max}$  in MFO, CCO and BPO are 0.670, 0.703 and 0.535, respectively. For AUPR, the best values in MFO, CCO and BPO are 0.674, 0.742 and 0.493, respectively. Similarly,  $S_{\min}$  achieves its optimal values in MFO, CCO BPO at 7.682, 9.072 and 36.138, respectively.

Furthermore, when only a single module is used, employing ss8 alone achieves the best AUPR scores, while Diamond alone performs best in terms of  $F_{\max}$ ; the performance of aa alone is not as impressive. A comparison between the aa+Diamond and ss8+Diamond combinations reveals a slight edge for the latter.

Lastly, while using the Diamond alignment score alone shows some effectiveness, it is particularly valuable in complementing the deficiencies of either the model-aa or model-ss8, thereby enhancing the overall prediction accuracy. Thus, sequence homology information remains a precious source for functional inference.

## Case analysis

In this section, we conduct two sets of case studies. The first case is a self-comparison, where we demonstrate the superiority of features extracted from secondary structures over those from primary sequences by predicting the function of Surface Lipoprotein Assembly Modifier (SLAM) proteins. It shows that features from secondary structures better reflect the key functional GO terms and exhibit better generalizability in non-homologous proteins. The second case involves a horizontal comparison with similar methods, by predicting the function of the LYP2\_MOUSE protein. It proves that our predictor accurately predicts all the bottom-layer functionalities of the protein with high scores, and provides deeper and more precise GO annotations. Following communication with users of protein function prediction software, their usage habits have been understood. For novel, unknown proteins, researchers typically focus on the top 20–30 high-scoring results of GO terms in each of the three sub-ontologies as a preliminary judgment of the most probable functions. Therefore, the threshold does not have an absolute significance. Hence, in the following cases, the threshold is only used as a reference value for filtering.

### Case 1, Prediction of non-homologous SLAM proteins

SLAM1 and SLAM2 are two transport membrane proteins of the *Neisseria meningitidis* serogroup. Their primary function is to transport substrates, with SLAM1 targeting TbpB, fHbp and LbpB, and SLAM2 targeting HpuA [54].

These two twin proteins are chosen as cases for several reasons. First, SLAM is not listed in the SwissProt database, thus not included in our training and testing sets. Secondly, homology comparisons of SLAM with other proteins in the SwissProt database yield a Diamond score of zero. This implies that SLAM is a non-homologous protein. Thirdly, the sequence variance between the two proteins is substantial, with only about 25% sequence identity (Supplementary Figure S5B). However, their secondary structures are remarkably similar, each comprising one  $\beta$  barrel and multiple  $\alpha$  helices (Supplementary Figure S5A), performing similar substrate transport functions. Therefore, these two SLAM cases effectively demonstrate that secondary-structure-based models are superior in predicting the function of non-homologous proteins with substantial sequence differences, compared with those primary-sequence-based models.

Three sets of tests are conducted using the aa+Diamond, ss8+Diamond and aa+ss8+Diamond models to predict SLAM1

and SLAM2, with MFO results at a threshold of 0.06 presented in Table 4. The aa+Diamond model predicts broader, higher-level GO terms, but the inclusion of ss8 features allows for the prediction of specific terms such as GO:0005215, GO:0022857, GO:0022803, related to transporter and transmembrane activity. To be noticed, within the aa+Diamond module, SLAM1 exhibits scores of 0.011 for both GO:0005215 and GO:0022857, placing it at the 31st and 32nd positions in the list. Generally, researchers do not focus on GO terms that are ranked too low. In addition, in the case of SLAM2, also in the aa+Diamond module, there were no detected GO terms associated with transporter activity. Despite the low sequence similarity between SLAM1 and SLAM2, these GO terms are predicted due to the ss8-model involvement, highlighting the transport-related functionalities essential to these proteins. Since SLAM proteins primarily act as substrate transporters, the highlighted parts in their functional annotations are particularly noteworthy.

This case validates the hypothesis proposed in Figure 1. Despite the vastly different arrangement of fibers and gravels, the function of the macrostructure can be determined as a 'bridge' rather than a 'tower' by learning the arrangement patterns of blocks. Similarly, even with the diversity in primary sequences, the accuracy of protein function prediction can be improved by learning the arrangement patterns of secondary structures. Incorporating features extracted from secondary structures provides higher sensitivity in predicting protein functions compared with models based solely on primary amino acid sequences. Even though the three main evaluation metrics ( $F_{\max}$ , AUPR,  $S_{\min}$ ) are indeed crucial for assessing the algorithm for general comparison, in a practical predicting application, it is vital to identify the specific key functions of an unknown protein. In this aspect, DeepSS2GO, which integrates secondary structure features, proves to be more effective.

### Case 2, Prediction of LYP2\_MOUSE protein

As the literature [46] has already examined the LYP2\_MOUSE protein (UniProt Symbol: Q9WTL7) and conducted comparisons with other similar algorithms, in this case, we also adapt this protein as our test object. The LYP2\_MOUSE protein serves as an acyl-protein thioesterase, responsible for hydrolyzing fatty acids attached to S-acylated cysteine residues in various proteins. A critical function of LYP2\_MOUSE includes facilitating the depalmitoylation process of zDHHC [55]. Therefore, predicting depalmitoylation-associated GO terms (GO:0098734 and GO:0002084) is of crucial importance in understanding its biological process.

Since the LYP2\_MOUSE protein exists in the SwissProt training set, we remove this protein from the set, then retrain the model using the same kernel and filter parameters as the optimal solution and predict this protein function with the new model. The BPO results are shown in Table 5. The DeepSS2GO algorithm successfully predicted all 23 GO terms with high scores, achieving an accuracy of 100%, highlighted in bold. Further analysis revealed that the success in predicting all GO terms mainly stemmed from accurately predicting the sub-node GO:0002084, which led to the inference of all parent-level label terms. Figure 4 compares the GO term labels predicted by DeepSS2GO with those by other similar algorithms. DeepSS2GO managed to accurately predict all labels, transcending all other same-type algorithms. This proves that our predictor provides deeper, more specific and crucial functional annotations, making it a more practical method for the accurate and comprehensive prediction of protein functions in biological research.

**Table 4:** Evaluation of MFO prediction for SLAM1 and SLAM2 proteins, using different combinations of DeepSS2GO modules with a threshold of 0.06

Methods	SLAM1			SLAM2		
	GO term	Annotation	Score	GO term	Annotation	Score
aa+D*	GO:0003674	molecular_function	0.368	GO:0003674	molecular_function	0.368
	GO:0003824	catalytic activity	0.235	GO:0003824	catalytic activity	0.362
	GO:0005488	binding	0.146	GO:0016787	hydrolase activity	0.133
	GO:0097159	organic cyclic compound binding	0.095	GO:0005488	binding	0.132
	GO:1901363	heterocyclic compound binding	0.091	GO:0097159	organic cyclic compound binding	0.079
	GO:0005515	protein binding	0.061	GO:0016757	glycosyltransferase activity	0.077
				GO:0016740	transferase activity	0.077
				GO:1901363	heterocyclic compound binding	0.070
ss8+D*	GO:0003674	molecular_function	0.355	GO:0003674	molecular_function	0.299
	GO:0005488	binding	0.355	GO:0005488	binding	0.287
	GO:0005515	protein binding	0.168	GO:0005515	protein binding	0.166
	<b>GO:0005215</b>	<b>transporter activity</b>	0.114	<b>GO:0005215</b>	<b>transporter activity</b>	0.137
	<b>GO:0022857</b>	<b>transmembrane transporter activity</b>	0.109	<b>GO:0022857</b>	<b>transmembrane transporter activity</b>	0.137
	GO:0003824	catalytic activity	0.062	<b>GO:0022803</b>	<b>passive transmembrane transporter</b>	0.092
	GO:0097159	organic cyclic compound binding	0.061	GO:0015267	channel activity	0.092
	GO:0003676	nucleic acid binding	0.060	GO:0003824	catalytic activity	0.083
	GO:1901363	heterocyclic compound binding	0.060	GO:0022829	wide pore channel activity	0.080
	GO:0140096	catalytic activity, acting on a protein	0.060	GO:0005102	signaling receptor binding	0.066
aa+ss8 +D*	GO:0003674	molecular_function	0.355	GO:0003674	molecular_function	0.341
	GO:0005488	binding	0.339	GO:0005488	binding	0.277
	GO:0005515	protein binding	0.159	GO:0005515	protein binding	0.154
	GO:0003824	catalytic activity	0.106	GO:0003824	catalytic activity	0.153
	<b>GO:0005215</b>	<b>transporter activity</b>	0.100	<b>GO:0005215</b>	<b>transporter activity</b>	0.118
	<b>GO:0022857</b>	<b>transmembrane transporter activity</b>	0.096	<b>GO:0022857</b>	<b>transmembrane transporter activity</b>	0.118
	GO:0097159	organic cyclic compound binding	0.074	GO:0016787	hydrolase activity	0.084
	GO:1901363	heterocyclic compound binding	0.064	<b>GO:0022803</b>	<b>passive transmembrane transporter</b>	0.079
	GO:0003676	nucleic acid binding	0.063	GO:0015267	channel activity	0.079
				GO:0022829	wide pore channel activity	0.069

Note: Under aa+D combination: SLAM1 has GO:0005215 and GO:0022857 scores of 0.011, ranking 31st and 32nd. SLAM2 has no transporter-related GO terms detected. Module D\* refers to the Diamond algorithm. The best results are in bold.

It is important to note that some GO terms in the literature [46] have been changed. For example, GO:0044260 is now obsolete, and GO:0044267 with GO:0006464 are secondary IDs for GO:0019538 and GO:0036211, respectively. Moreover, in the latest GO database used in this study, GO:0006807, GO:1901564 and GO:1901565 are defined as parent-level terms of GO:0002084 [56]. The following four aspects are continuously updated: the SwissProt database, the GO database, the interrelationships between GO terms and the correspondence between proteins and GO terms. Therefore, the simplicity, time efficiency and ease of retraining the DeepSS2GO model ensure regular updates.

These results indicate that the proposed DeepSS2GO method outperforms the state-of-the-art methods in stability, reliability, accuracy, efficiency and generalization to non-homologous proteins. It can further extend to proteins of species not 'seen' in the training set, predicting biological functions of new and unknown protein sequences.

## DISCUSSION

Protein function prediction methods based on primary sequences or tertiary structures exhibit inherent limitations. The information in primary sequences contains an overload of information, making it challenging to accurately predict functions from unknown species through amino acid sequence information alone. Although leveraging tertiary structure for function prediction improves accuracy, it is impractical for analyzing massive

datasets due to its time-consuming nature. From primary to tertiary levels, it is precisely because the 'functional information density' continually increases that it becomes easier to predict function. This functional information density refers to the ratio of functional information to total information. Considering this, our developed secondary-structure-based prediction algorithm, DeepSS2GO, can compensate for these shortcomings, combining the efficiency of sequencing based on primary sequences with the accuracy of utilizing partial spatial structural information.

DeepSS2GO is characterized by its accuracy, critical insights, comprehensiveness, efficiency and ease of updating. It enhances protein function prediction by reducing the redundant information of primary sequences through the modular integration of secondary structure features. This approach improves the prediction accuracy, relevancy and breadth. Furthermore, DeepSS2GO outperforms current leading sequence-based predictors in performance, offering comprehensive predictions of essential protein functions and demonstrating excellent generalization capabilities for non-homologous proteins and new species. Its rapid prediction capability makes it highly applicable in various fields, including metagenomics, for large-scale unknown species. Additionally, the user-friendly model architecture minimizes the costs associated with retraining, facilitating quicker and more convenient updates with the latest database.

However, there are areas where DeepSS2GO can be further improved. In an effort to emphasize the effectiveness of the secondary structure, the model was built using the classic

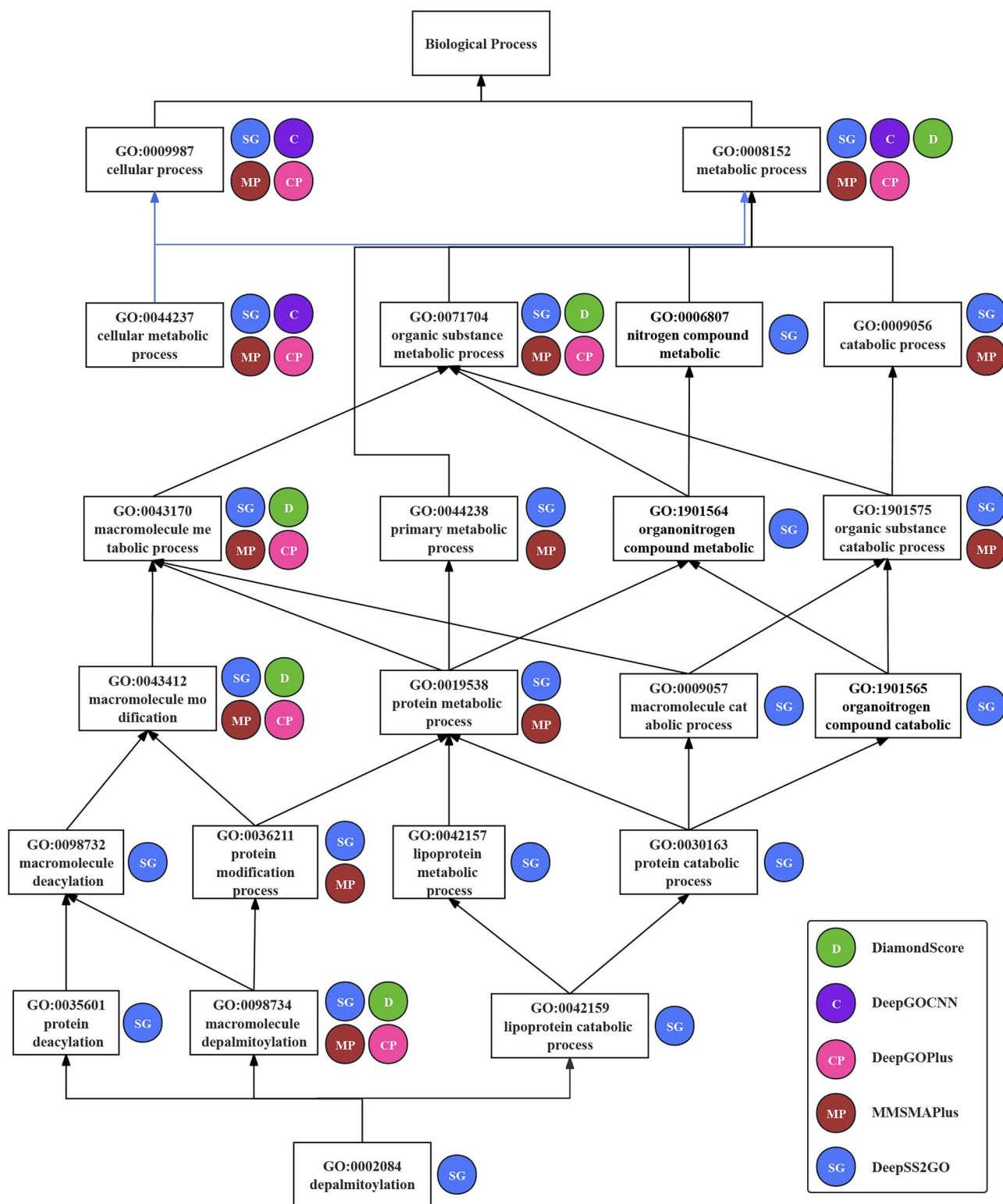


**Figure 4.** Comparison of predicted GO terms by various methods for LYPA2\_MOUSE (UniProt Symbol: Q9WTL7) protein within the BPO DAG. The established baseline for these predictions is derived from the propagation of experimental BPO annotations (GO:0002084).

conventional CNN, proving that even simple methods can yield outstanding results. Recent algorithmic developments in areas such as GNN [18], Diffusion mechanisms [45], Geometric Deep Learning [57], Self-supervised learning [48] and Large Language Models [22] have shown exceptional utility in protein structure and function analysis. Applying these state-of-the-art algorithms

to extract protein sequence information from various dimensions could enhance the accuracy of functional predictions. Moreover, the algorithm transition from primary to secondary sequence prediction uses ProtTrans and ESM pre-trained models, which are limited by protein sequence length, thereby excluding large proteins over 1024 amino acids. Adopting more versatile

**Table 5:** Evaluation of the BPO prediction for the LYPA2\_MOUSE protein, ranked in descending order of scores

GO term	Annotation	Score
<b>GO:0008150</b>	biological_process	0.870
<b>GO:0008152</b>	metabolic process	0.823
<b>GO:0071704</b>	organic substance metabolic process	0.814
<b>GO:0009987</b>	cellular process	0.781
<b>GO:0044238</b>	primary metabolic process	0.766
<b>GO:0043170</b>	macromolecule metabolic process	0.663
<b>GO:0043412</b>	macromolecule modification	0.663
<b>GO:0098732</b>	macromolecule deacylation	0.663
<b>GO:0006807</b>	nitrogen compound metabolic	0.654
<b>GO:0019538</b>	protein metabolic process	0.654
<b>GO:0035601</b>	protein deacylation	0.654
<b>GO:0036211</b>	protein modification process	0.654
<b>GO:1901564</b>	organonitrogen compound metabolic	0.654
<b>GO:0009056</b>	catabolic process	0.618
<b>GO:1901575</b>	organic substance catabolic process	0.614
<b>GO:0042157</b>	lipoprotein metabolic process	0.538
<b>GO:0098734</b>	macromolecule depalmitoylation	0.495
<b>GO:0044237</b>	cellular metabolic process	0.484
<b>GO:1901565</b>	organonitrogen compound catabolic	0.481
<b>GO:0009057</b>	macromolecule catabolic process	0.446
GO:0050896*	response to stimulus	0.444
<b>GO:0030163</b>	protein catabolic process	0.438
GO:0006629*	lipid metabolic process	0.413
GO:0044255*	cellular lipid metabolic process	0.413
GO:0046486*	glycerolipid metabolic process	0.413
<b>GO:0002084</b>	protein depalmitoylation	0.389
<b>GO:0042159</b>	lipoprotein catabolic process	0.389

Note: GO terms in bold are True Position predictions. Go terms with \* are referred to as False Positive predictions.

secondary structure prediction methods for longer sequences in the future would expand our algorithm scope significantly. Lastly, functional prediction is not limited to full-length proteins but can also be applied to studying various polypeptides [58, 59], integrating multiple features which will facilitate a broader elucidation of disease mechanisms and the discovery of drug targets. Therefore, we aim to further integrate drug and disease information using information fusion methods, allowing functional annotation algorithms to be more effectively applied in practical applications, benefiting humanity.

Overall, DeepSS2GO combines advanced feature learning capabilities with cross-species transfer potential. As genomic sequencing progresses and the quantity of new species sequence data grows, this method promises to be a valuable tool for protein function prediction, balancing accuracy with computational efficiency.

#### Key Points

- DeepSS2GO is a protein function predictor that treats secondary structure as a module, integrating it with primary sequence and homology information.
- DeepSS2GO combines sequence-based speed with structure-based accuracy, also simplifying redundant information in primary sequences and avoiding time-consuming complexities associated with tertiary structure analysis.
- DeepSS2GO surpasses similar algorithms in accuracy, capable of predicting key functions of non-homologous

proteins and providing more in-depth and specific functional annotations.

- DeepSS2GO exhibits exceptional performance and speed, operating five times faster than advanced algorithms, making it more suitable for large-scale sequencing data.
- DeepSS2GO model is streamlined, enabling easy updates and the tracking of the latest SwissProt and GO databases.

## SUPPLEMENTARY DATA

Supplementary data are available online at <http://bib.oxfordjournals.org/>.

## ACKNOWLEDGMENTS

The authors thank the HPC-Service Station, Cryo-EM Center and Center for Computational Science and Engineering at Southern University of Science and Technology. M.L. is an investigator of SUSTech Institute for Biological Electron Microscopy.

## AUTHOR CONTRIBUTIONS STATEMENT

F.S., M.N. and M.L. conceived and supervised the whole project. F.S. programmed the code and wrote the manuscript. J.S. performed data processing and analyzed the results. S.H. and N.Z. refined the algorithm and reviewed the manuscript. K.L. processed the case study. All the authors discussed, revised and proofread the manuscript.

## DATA AVAILABILITY

The source code and trained models are available for research and non-commercial use at <https://github.com/orca233/DeepSS2GO>.

## REFERENCES

1. Berrar D, Dubitzky W. Deep learning in bioinformatics and biomedicine. *Brief Bioinform* 2021;**22**(2):1513–4.
2. Kustatscher G, Collins T, Gingras A-C, et al. Understudied proteins: opportunities and challenges for functional proteomics. *Nat Methods* 2022;**19**(7):774–9.
3. Fa R, Cozzetto D, Wan C, Jones DT. Predicting human protein function with multi-task deep neural networks. *PLoS One* 2018;**13**(6):e0198216.
4. Ashburner M, Ball CA, Blake JA, et al. Gene ontology: tool for the unification of biology. *Nat Genet* 2000;**25**(1):25–9.
5. Bairoch A. The enzyme database in 2000. *Nucleic Acids Res* 2000;**28**(1):304–5.
6. Kanehisa M, Goto S. KEGG: Kyoto encyclopedia of genes and genomes. *Nucleic Acids Res* 2000;**28**(1):27–30.
7. Mistry J, Chuguransky S, Williams L, et al. Pfam: the protein families database in 2021. *Nucleic Acids Res* 2021;**49**(D1):D412–9.
8. Bileschi ML, Belanger D, Bryant DH, et al. Using deep learning to annotate the protein universe. *Nat Biotechnol* 2022;**40**(6):932–7.
9. Min S, Lee B, Yoon S. Deep learning in bioinformatics. *Brief Bioinform* 2017;**18**(5):851–69.
10. Webb S, et al. Deep learning for biology. *Nature* 2018;**554**(7693):555–7.

11. Bernhofer M, Dallago C, Karl T, et al. Predictprotein-predicting protein structure and function for 29 years. *Nucleic Acids Res* 2021;**49**(W1):W535–40.
12. Camacho C, Coulouris G, Avagyan V, et al. Blast+: architecture and applications. *BMC Bioinformatics* 2009;**10**:1–9.
13. Altschul SF, Madden TL, Schäffer AA, et al. Gapped blast and psi-blast: a new generation of protein database search programs. *Nucleic Acids Res* 1997;**25**(17):3389–402.
14. Blum M, Chang H-Y, Chuguransky S, et al. The interpro protein families and domains database: 20 years on. *Nucleic Acids Res* 2021;**49**(D1):D344–54.
15. Edgar RC, Batzoglou S. Multiple sequence alignment. *Curr Opin Struct Biol* 2006;**16**(3):368–73.
16. Jeong JC, Lin X, Chen X-W. On position-specific scoring matrix for protein function prediction. *IEEE/ACM Trans Comput Biol Bioinform* 2010;**8**(2):308–15.
17. Jianxin W. Introduction to convolutional neural networks. *National key lab for novel software technology. Nanjing University China* 2017;**5**(23):495.
18. Sanchez-Lengeling B, Reif E, Pearce A, Wiltschko AB. A gentle introduction to graph neural networks. *Distill* 2021;**6**(9):e33.
19. Ho J, Jain A, Abbeel P. Denoising diffusion probabilistic models. *Advances in neural information processing systems* 2020;**33**:6840–51.
20. Vaswani A, Shazeer N, Parmar N, et al. Attention is all you need. *Advances in neural information processing systems* 2017;**30**.
21. Rao RM, Meier J, Sercu T, et al. Transformer protein language models are unsupervised structure learners. *bioRxiv* 2020.
22. Madani A, Krause B, Greene ER, et al. Large language models generate functional protein sequences across diverse families. *Nat Biotechnol* 2023;**41**:1099–106.
23. Zeng M, Zhang F, Fang-Xiang W, et al. Protein–protein interaction site prediction through combining local and global features with deep neural networks. *Bioinformatics* 2020;**36**(4):1114–20.
24. Kulmanov M, Hoehndorf R. Deepgoplus: improved protein function prediction from sequence. *Bioinformatics* 2020;**36**(2):422–9.
25. Cao Y, Shen Y. Tale: transformer-based protein function annotation with joint sequence–label embedding. *Bioinformatics* 2021;**37**(18):2825–33.
26. Fan K, Guan Y, Zhang Y. Graph2go: a multi-modal attributed network embedding method for inferring protein functions. *GigaScience* 2020;**9**(8):giaa081.
27. Vladimir Gligorijević P, Renfrew D, Kosciolk T, et al. Structure-based protein function prediction using graph convolutional networks. *Nat Commun* 2021;**12**.
28. You R, Yao S, Xiong Y, et al. Netgo: improving large-scale protein function prediction with massive network information. *Nucleic Acids Res* 2019;**47**(W1):W379–87.
29. Szklarczyk D, Gable AL, Nastou KC, et al. The string database in 2021: customizable protein–protein networks, and functional characterization of user-uploaded gene/measurement sets. *Nucleic Acids Res* 2021;**49**(D1):D605–12.
30. You R, Yao S, Mamitsuka H, Zhu S. Deepgraphgo: graph neural network for large-scale, multispecies protein function prediction. *Bioinformatics* 2021;**37**(Supplement\_1):i262–71.
31. Anfinsen CB. Principles that govern the folding of protein chains. *Science* 1973;**181**(4096):223–30.
32. Chayen NE, Saridakis E. Protein crystallization: from purified protein to diffraction-quality crystal. *Nat Methods* 2008;**5**(2):147–53.
33. Yip KM, Fischer N, Paknia E, et al. Atomic-resolution protein structure determination by cryo-em. *Nature* 2020;**587**(7832):157–61.
34. Jeffery CJ. Current successes and remaining challenges in protein function prediction. *Front Bioinf* 2023;**3**:1222182.
35. Renaud J-P, Chari A, Ciferri C, et al. Cryo-em in drug discovery: achievements, limitations and prospects. *Nat Rev Drug Discov* 2018;**17**(7):471–92.
36. Jumper J, Evans R, Pritzel A, et al. Highly accurate protein structure prediction with alphafold. *Nature* 2021;**596**(7873):583–9.
37. Zongyang D, Hong S, Wang W, et al. The trrosetta server for fast and accurate protein structure prediction. *Nat Protoc* 2021;**16**(12):5634–51.
38. Touw WG, Baakman C, Black J, et al. A series of pdb-related data-banks for everyday needs. *Nucleic Acids Res* 2015;**43**(D1):D364–8.
39. Kabsch W, Sander C. Dictionary of protein secondary structure: pattern recognition of hydrogen-bonded and geometrical features. *Biopolymers* 1983;**22**(12):2577–637.
40. Lai B, Jinbo X. Accurate protein function prediction via graph attention networks with predicted structure information. *Brief Bioinform* 2022;**23**.
41. Yang Z, Tsui SK-W. Functional annotation of proteins encoded by the minimal bacterial genome based on secondary structure element alignment. *J Proteome Res* 2018;**17**(7):2511–20.
42. Singh J, Paliwal K, Litfin T, et al. Reaching alignment-profile-based accuracy in predicting protein secondary and tertiary structural properties without alignment. *Sci Rep* 2022;**12**(1):7607.
43. Tesei G, Trolle AI, Jonsson N, et al. Conformational ensembles of the human intrinsically disordered proteome. *Nature* 2024;**626**(8000):897–904.
44. Buchfink B, Xie C, Huson DH. Fast and sensitive protein alignment using diamond. *Nat Methods* 2015;**12**(1):59–60.
45. Yuan Q, Xie J, Xie J, et al. Fast and accurate protein function prediction from sequence through pretrained language model and homology-based label diffusion. *Brief Bioinform* 2023;**24**.
46. Wang Z, Deng Z, Zhang W, et al. Mmsmaplus: a multi-view multi-scale multi-attention embedding model for protein function prediction. *Brief Bioinform* 2023;bbad201.
47. Uniprot: the universal protein knowledgebase in 2021. *Nucleic Acids Res* 2021;**49**(D1):D480–9.
48. Elnaggar A, Heinzinger M, Dallago C, et al. Prottrans: toward understanding the language of life through self-supervised learning. *IEEE Trans Pattern Anal Mach Intell* 2021;**44**(10):7112–27.
49. ADAM Paszke, SAM Gross, FRANCISCO Massa, ADAM Lerer, JAMES Bradbury, GREGORY Chanan, TREVOR Killeen, ZEMING Lin, NATALIA Gimelshein, LUCA Antiga, ALBAN Desmaison, ANDREAS Kopf, EDWARD Yang, ZACHARY DeVito, MARTIN Raison, ALYKHAN Tejani, SASANK Chilamkurthy, Benoit Steiner, LU Fang, JUNJIE BAI, and SOUMITH Chintala. Pytorch: An imperative style, high-performance deep learning library. In H. Wallach, H. Larochelle, A. Beygelzimer, F. Dalché-Buc, E. Fox, and R. Garnett, editors, *Advances in Neural Information Processing Systems*, volume **32**. Curran Associates, Inc., 2019.
50. Kingma, Jimmy BA. Adam: a method for stochastic optimization. *arXiv preprint arXiv:1412.6980* 2014.
51. Radivojac P, Clark WT, Oron TR, et al. A large-scale evaluation of computational protein function prediction. *Nat Methods* 2013;**10**(3):221–7.
52. Clark WT, Radivojac P. Information-theoretic evaluation of predicted ontological annotations. *Bioinformatics* 2013;**29**(13):i53–61.
53. JESSE Davis and MARK Goadrich. The relationship between precision-recall and roc curves. In *Proceedings of the 23rd international conference on Machine learning*, pages 233–240, 2006.

54. Hooda Y, Lai CC-L, Judd A, et al. Slam is an outer membrane protein that is required for the surface display of lipidated virulence factors in neisseria. *Nat Microbiol* 2016;**1**(4): 1–9.
55. Milde S, Coleman MP. Identification of palmitoyltransferase and thioesterase enzymes that control the subcellular localization of axon survival factor nicotinamide mononucleotide adenylyltransferase 2 (nmnat2). *J Biol Chem* 2014;**289**(47): 32858–70.
56. Quickgo go:0002084. <https://www.ebi.ac.uk/QuickGO/term/GO:0002084>, 2023. (10 December 2023, date last accessed).
57. Gainza P, Sverrisson F, Monti F, et al. Deciphering interaction fingerprints from protein molecular surfaces using geometric deep learning. *Nat Methods* 2020;**17**(2):184–92.
58. Kim D-I, Han S-H, Park H, et al. Pseudo-isolated  $\alpha$ -helix platform for the recognition of deep and narrow targets. *J Am Chem Soc* 2022;**144**(34):15519–28.
59. Thakur A, Sharma A, Alajangi HK, et al. In pursuit of next-generation therapeutics: antimicrobial peptides against superbugs, their sources, mechanism of action, nanotechnology-based delivery, and clinical applications. *Int J Biol Macromol* 2022;**218**:135–56.